Materials Advances

Electronic Supplementary Information

A near-infrared intelligent molecular rotor with aggregation induced-emission toward viscosity detection of liquids

Lingfeng Xu[1,2,*], Yanrong Huang[3], Xinkang Peng[1], Kui Wu[4], Chunfang Huang[1], Limin Liu [1,*]

1 School of Chemistry and Chemical Engineering, Jinggangshan University, Ji'an, Jiangxi 343009, China

2 State Key Laboratory of Luminescent Materials & Devices, Guangdong Provincial Key Laboratory of Luminescence from Molecular Aggregates, College of Materials Science & Engineering, South China University of Technology, Guangzhou 510640, China

3 School of Food Science and Engineering, Guangdong Province Key Laboratory for Green Processing of Natural Products and Product Safety, South China University of Technology, Guangzhou 510640, China

4 Fine Chemical Industry Research Institute, School of Chemistry, Sun Yat-sen University, Guangzhou 510275, China

[*] *Corresponding author. E-mail: rs7lfxu@outlook.com.*

E-mail: llm24@126.com.

Table of contents

Experimental section

1. Synthesis procedure

Synthesis of 4-bromo-2,6-dimethoxybenzaldehyde (Compound 1)

4-bromo-2,6-dihydroxybenzaldehyde (217 mg, 1.0 mM) was dissolved in a round-bottom flask containing acetonitrile, and the potassium carbonate (276.0 mg, 2 mM) was added into upon flask, under the protection of nitrogen, then stirred under ambient temperature for 1 h. Afterwards, the bromomethane (142.5 mg, 1.5 mM) was dissolved in the acetonitrile as well, and injected into upon mixture slowly through the syringe. The reaction system was stirred under 45 °C overnight. After cooling to room temperature, the solvent was removed, and washed with distilled water for three times. The mixture was dried with Na_2SO_4, and further purified through the silica gel column chromatography using DCM/ petroleum ether (v/v=1/1) to afford the Compound 1 (186.2 mg, 76%). ^{1}H NMR (400 MHz, $CDCl_3$) δ 10.44 (s, 1H), 6.77 (s, 2H), 3.91 (s, 6H); ^{13}C NMR (101 MHz, $CDCl_3$) δ 188.54, 162.30, 130.32, 113.02, 107.92, 56.44. MS (ESI): m/z 244.98157 $[M]^+$, calcd for $C_9H_9BrO_3$ 245.07200.

Synthesis of (4-(diphenylamino)phenyl)boronic acid (Compound 2)

The diphenylamine (169.0 mg, 1.0 mM) was dissolved in acetonitrile, and the potassium carbonate (414.0 mg, 3.0 mM) was added into upon solution as well. Then the mixture was stirred under ambient temperature for over an hour under N_2 atmosphere. Afterwards, the (4-bromophenyl)boronic (200.0 mg, 1.0 mM) solution was added into upon mixture slowly, and the reaction system was refluxed at 81 °C overnight, and the reaction was monitored by TLC. After cooling down to room

temperature, the solvent was removed, the crude product obtained was purified through the silica-gel column chromatography using DCM/petroleum ether (v/v=2/1), Compound 2 as light yellow powder was obtained (196.62 mg, 68%). ^{1}H NMR (600 MHz, $CDCl_3$) δ 7.72 (dd, J = 26.0, 7.9 Hz, 4H), 7.30 (d, J = 7.5 Hz, 6H), 6.92 (dd, J = 23.5, 7.8 Hz, 4H), 2.51 (s, 2H); ^{13}C NMR (101 MHz, $CDCl_3$) δ 151.69, 147.17, 136.75, 129.46, 125.47, 123.84, 121.01. MS (ESI): m/z 290.13496 $[M+H]^+$, calcd for $C_{18}H_{16}BNO_2$ 289.14100.

Synthesis of 4'-(diphenylamino)-3,5-dimethoxy-[1,1'-biphenyl]-4-carbaldehyde (Compound 3)

To the solution of Compound 1 (245.0 mg, 1.0 mM), Compound 2 (290.1 mg, 1.0 mM) was added into upon solution, and the potassium carbonate aqueous solution (2 M) and TBAB (161.2 mg, 0.5 mol) was dropped into the above solution as well, followed with continuous stirring at room temperature under N_2 atmosphere for an hour. Then the solution of palladium acetate (4.4 mg, 0.02 mmol) was added dropwise to upon mixture. Afterwards, the reaction system was refluxed overnight, and the reaction was monitored by Thin Layer Chromatography (TLC). After the reaction was over, the solvent was removed through rotary evaporation. The residual was washed with the saturated salt water, the organic phase was collected and dried over $MgSO_4$. Finally, the crude product was purified by the silica-gel column chromatography using DCM/methanol (v/v=3/1) to afford the Compound 3 as a yellow powder (323.51 mg, 79%). ^{1}H NMR (600 MHz, $CDCl_3$) δ 10.53 (s, 1H), 7.50 (d, J = 8.4 Hz, 2H), 7.32 (d, J = 7.7 Hz, 2H), 7.16 (d, J = 7.6 Hz, 6H), 7.09 (t, J = 7.3 Hz, 2H), 6.76 (d, J = 8.1 Hz, 4H), 3.98 (s, 6H); ^{13}C NMR

(101 MHz, $CDCl_3$) δ 189.00, 162.50, 148.71, 148.62, 147.27, 133.43, 129.46, 127.99, 124.85, 123.55, 122.99, 107.93, 102.21, 56.12. MS (ESI): m/z 410.17377 $[M+H]^+$, calcd for $C_{27}H_{23}NO_3$ 409.16779.

Synthesis of 1-ethyl-4-methylquinolin-1-ium (Compound 4)

A mixture of 4-methylquinoline (143.0 mg, 1.0 mM) and bromoethane (90.0 μL, 1.2 mM) in toluene were stirred under room temperature for 10 min, and then the solution was refluxed in the dark under N_2 atmosphere overnight. The reaction was monitored by thin layer chromatography (TLC). After that, the resultant reaction system was cooled to temperature, and then the solvent was removed in *vacuo*. The crude product was purified *via* silica-gel column chromatography using CH_2Cl_2/CH_3OH (v/v=2/1) to afford Compound 4 as a grey white solid (130.7 mg, 76%). ^1H NMR (600 MHz, MeOD) δ 9.00 (d, J = 8.6 Hz, 1H), 8.58 (d, J = 9.1 Hz, 1H), 8.37 (d, J = 8.1 Hz, 1H), 8.25 (t, J = 7.4 Hz, 1H), 8.03 (d, J = 8.6 Hz, 1H), 5.08 (q, J = 7.3 Hz, 2H), 3.17 (s, 3H), 1.68 (t, J = 7.3 Hz, 3H); ^{13}C NMR (101 MHz, $CDCl_3$) δ 158.08, 148.54, 136.76, 135.74, 130.08, 129.34, 126.91, 123.31, 119.07, 53.30, 20.58, 15.93. MS (ESI): m/z 172.11231 $[M]^+$, calcd for $C_{12}H_{14}N^+$ 172.11208.

Synthesis of 4-(2-(4'-(diphenylamino)-3,5-dimethoxy-[1,1'-biphenyl]-4-yl)vinyl)-1-ethylquinolin-1-ium (molecular rotor DPADQ)

Compound 4 (172.1 mg, 1.0 mM) dissolved in methanol was added, and the Compound 3 (410.2 mg, 1.0 mM) solution was dissolved in methanol as well. The mixture was stirred under room temperature for half an hour under N_2 atmosphere. Then the reaction system was refluxed at 65 °C, during the reaction process, the solution of pyridine (80

μL, 1 mmol) in methanol was injected dropwise into the above mixture by syringe, and the reaction was monitored by TLC. When the reaction was finished, the solvent was removed under reduce pressure, the crude product obtained was purified through the silica-gel column chromatography using DCM/methanol (v/v=6/1), and the molecular rotor DPADQ as a dark red solid was obtained (444.9 mg, 79%). ^{1}H NMR (600 MHz, CD_3CN) δ 8.94 (d, J = 6.6 Hz, 1H), 8.65 (dd, J = 27.4, 12.3 Hz, 2H), 8.37-8.31 (m, 2H), 8.04-7.97 (m, 1H), 7.73 (d, J = 8.6 Hz, 2H), 7.43-7.33 (m, 5H), 7.13 (t, J = 8.9 Hz, 8H), 7.00 (d, J = 9.7 Hz, 2H), 4.92 (q, J = 7.2 Hz, 2H), 4.10 (s, 6H), 1.67 (t, J = 7.2 Hz, 3H); ^{13}C NMR (101 MHz, DMSO-d_6) δ 160.47, 154.55, 147.59, 147.26, 144.46, 141.36, 140.57, 138.00, 135.50, 130.19, 128.65, 126.95, 126.57, 125.86, 124.86, 124.09, 123.14, 122.03, 116.53, 111.66, 102.62, 56.85, 52.52, 15.62. MS (ESI): m/z 563.27031 $[M]^+$, calcd for $C_{39}H_{35}N_2O_2^+$ 563.26930.

2. The Förster–Hoffmann equation

According to the previous studies,[1] the relationship between the fluorescence intensity of the molecular rotor DPADQ and the viscosity can be determined by the following Förster–Hoffmann equation:

$$\log I = C + x \log \eta \qquad (1)$$

where η represents the viscosity, I represents the fluorescence intensity of the molecular rotor DPADQ at 725 nm, C is a constant, and x represents the sensitivity of the molecular rotor towards viscosity.

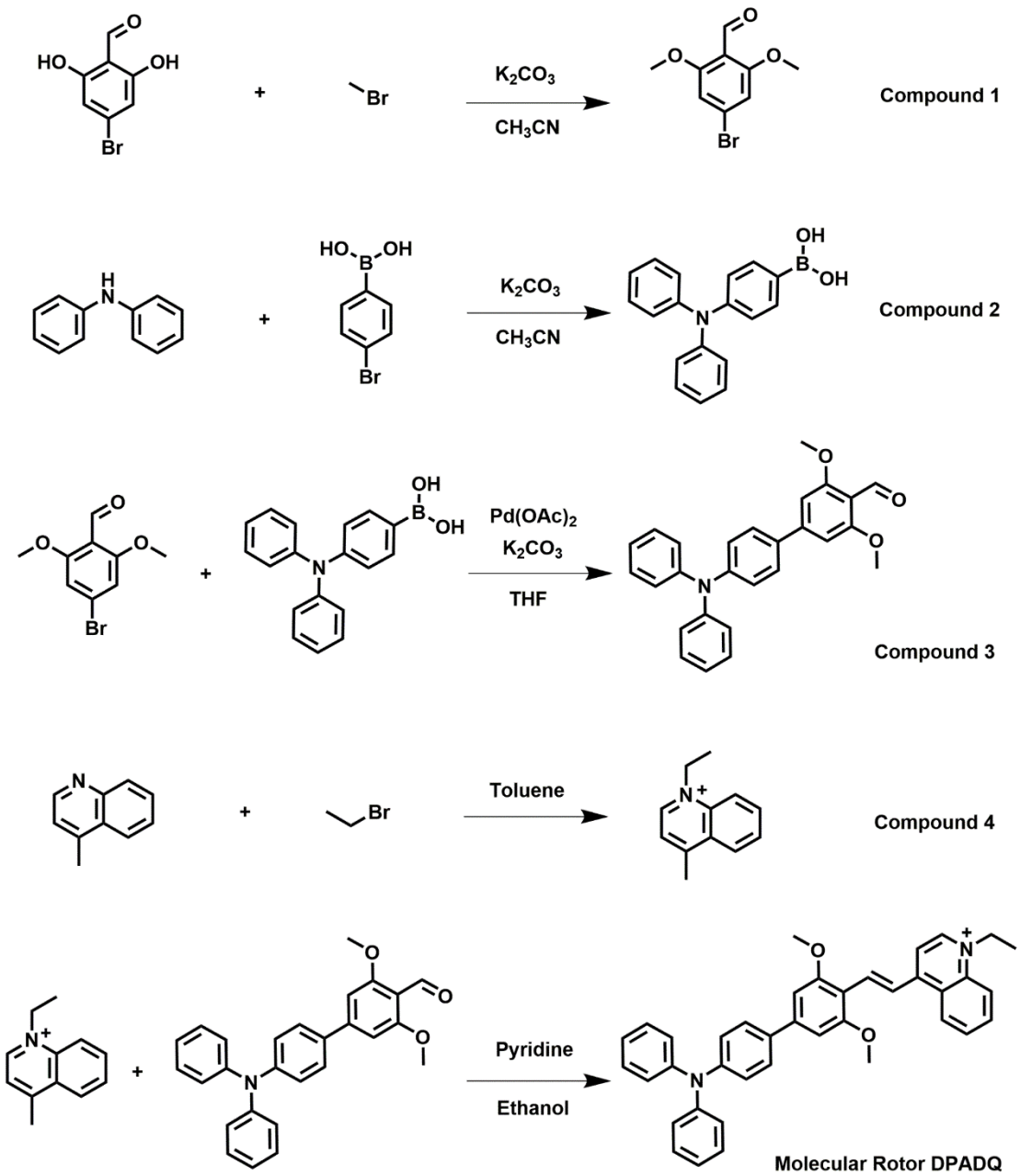

Scheme S1. Synthesis route for the molecular rotor DPADQ.

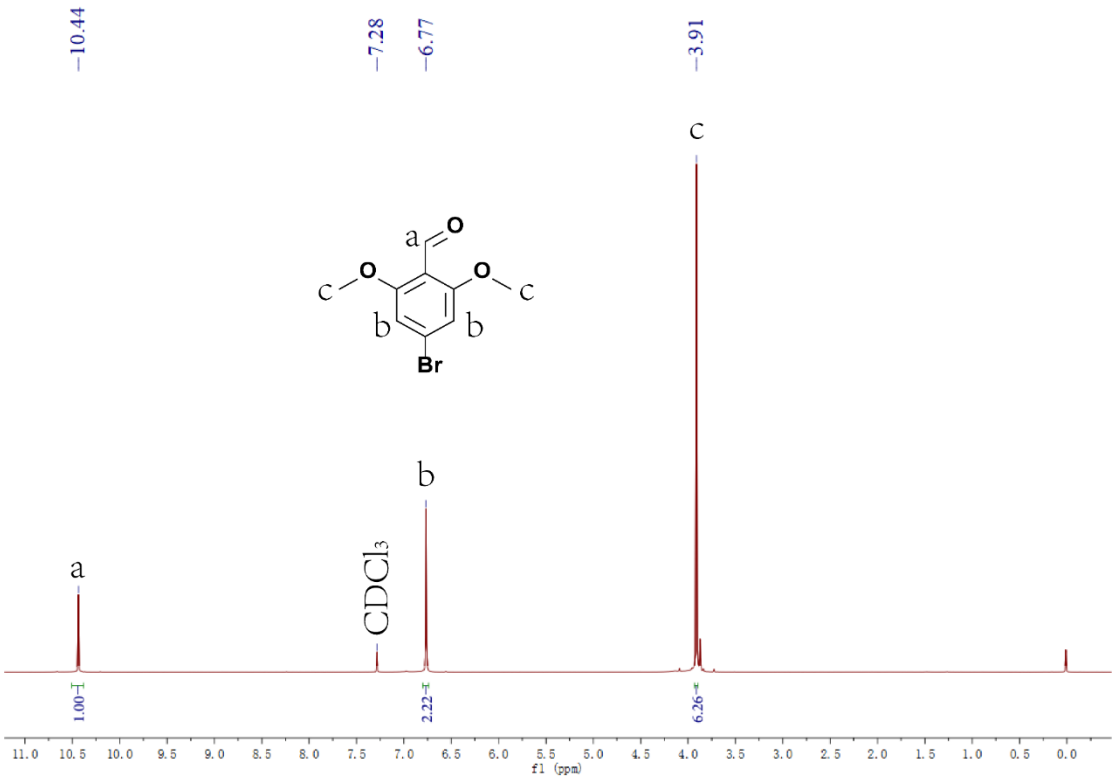

Fig. S1 ^{1}H-NMR spectrum of Compound 1 in $CDCl_3$.

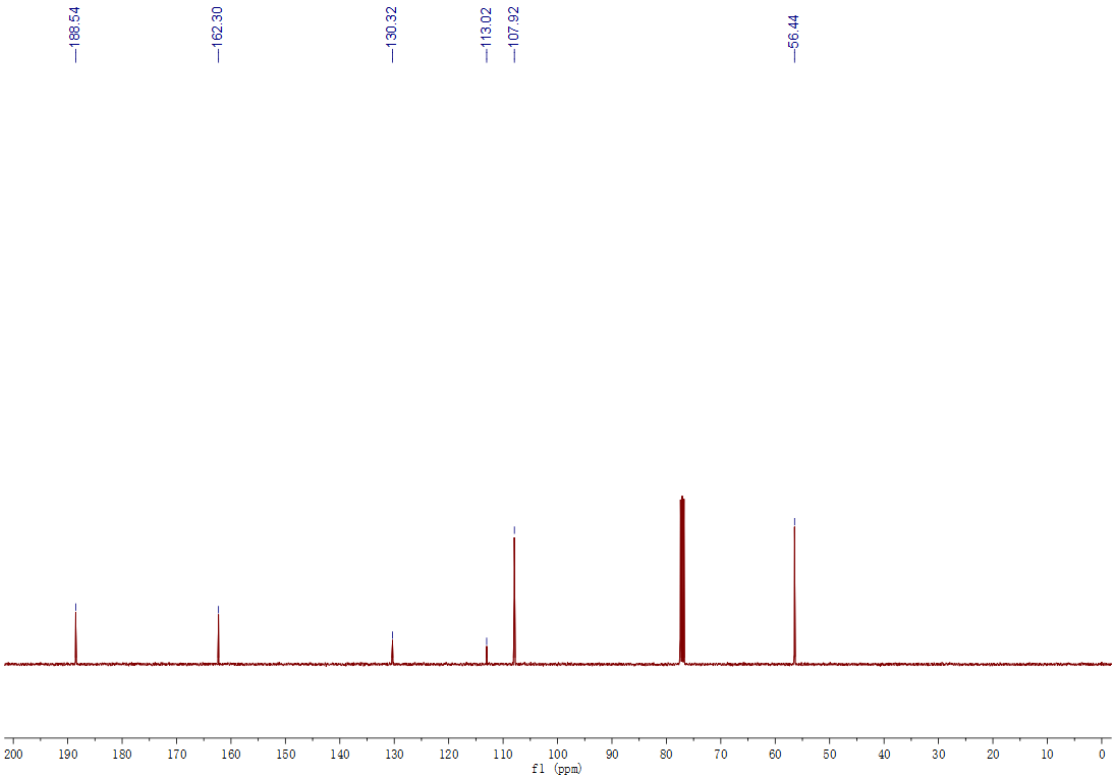

Fig. S2 ^{13}C-NMR spectrum of Compound 1 in $CDCl_3$.

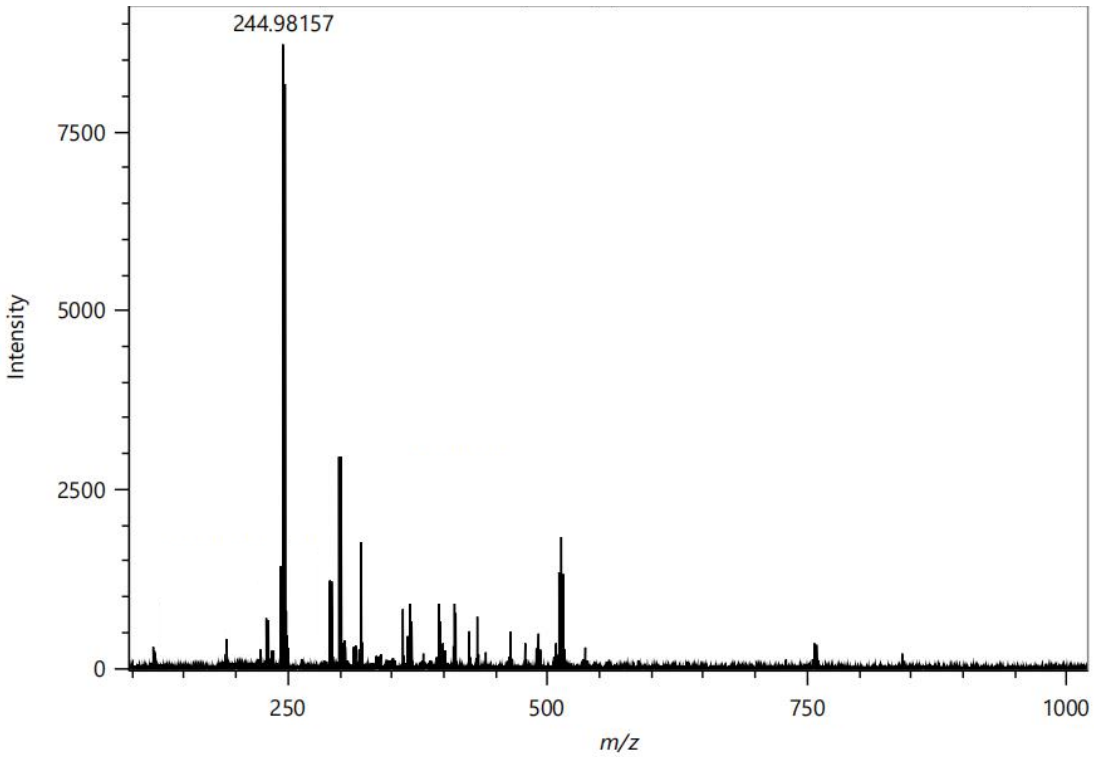

Fig. S3 HR mass spectrum of Compound 1. MS (ESI): m/z 244.98157 $[M]^+$.

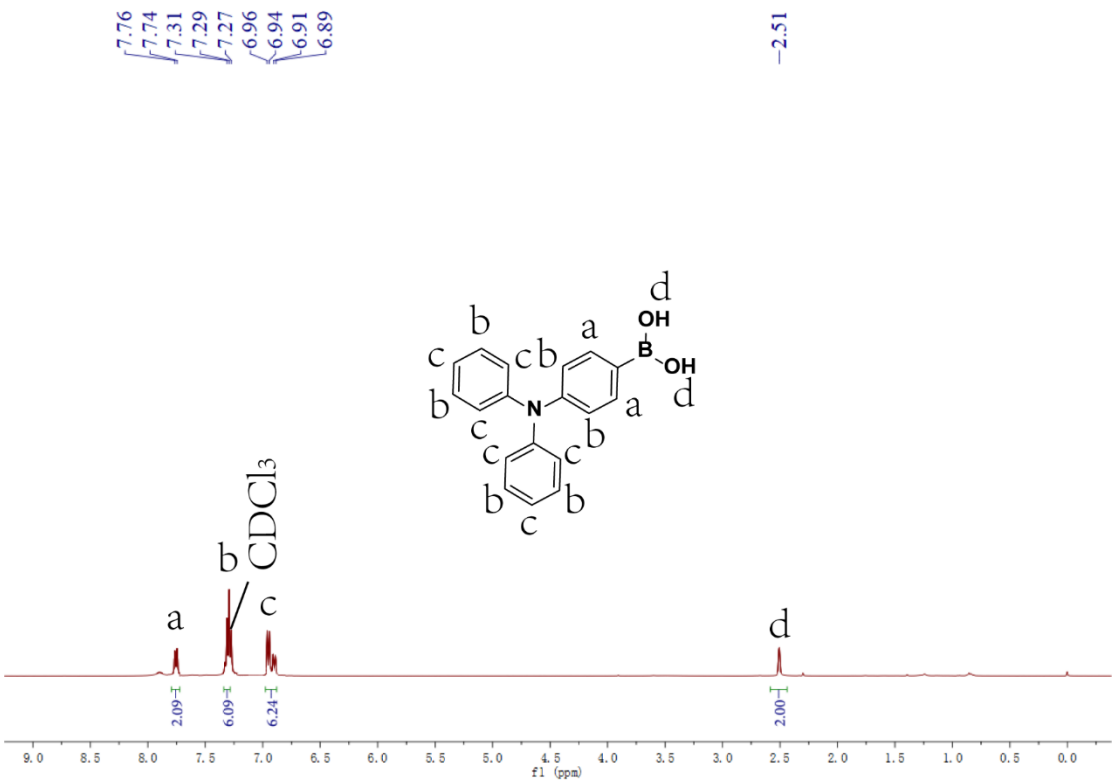

Fig. S4 ^{1}H-NMR spectrum of Compound 2 in $CDCl_3$.

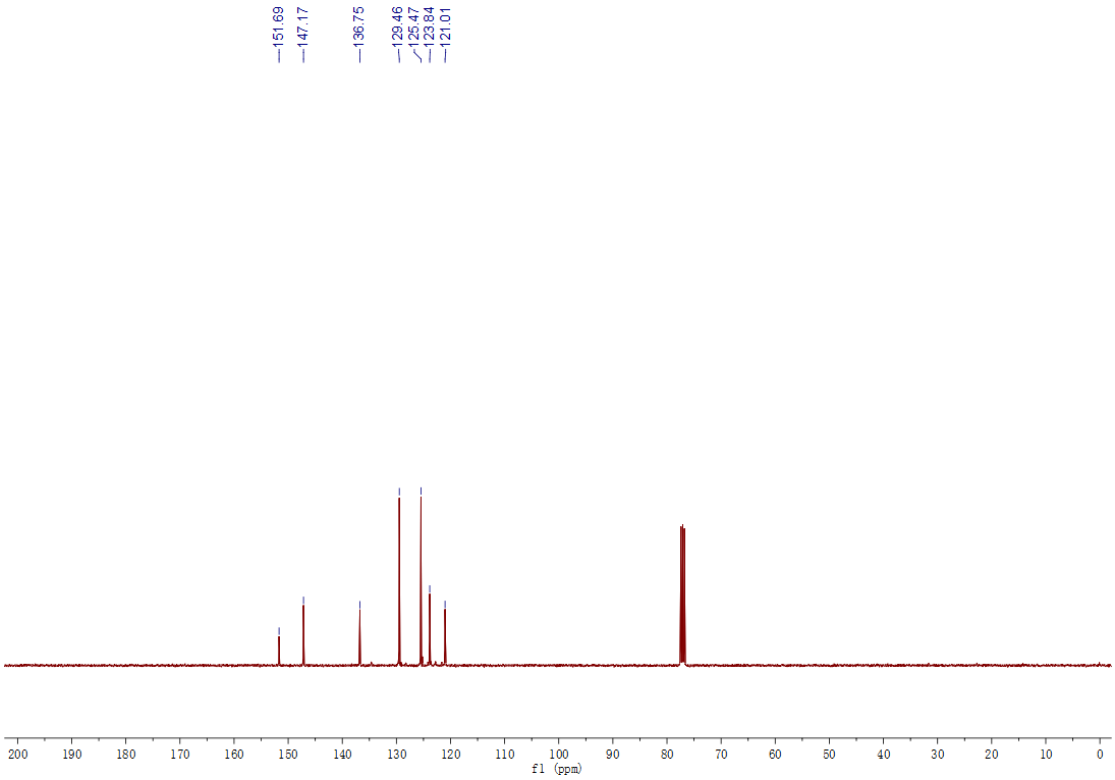

Fig. S5 ^{13}C-NMR spectrum of Compound 2 in $CDCl_3$.

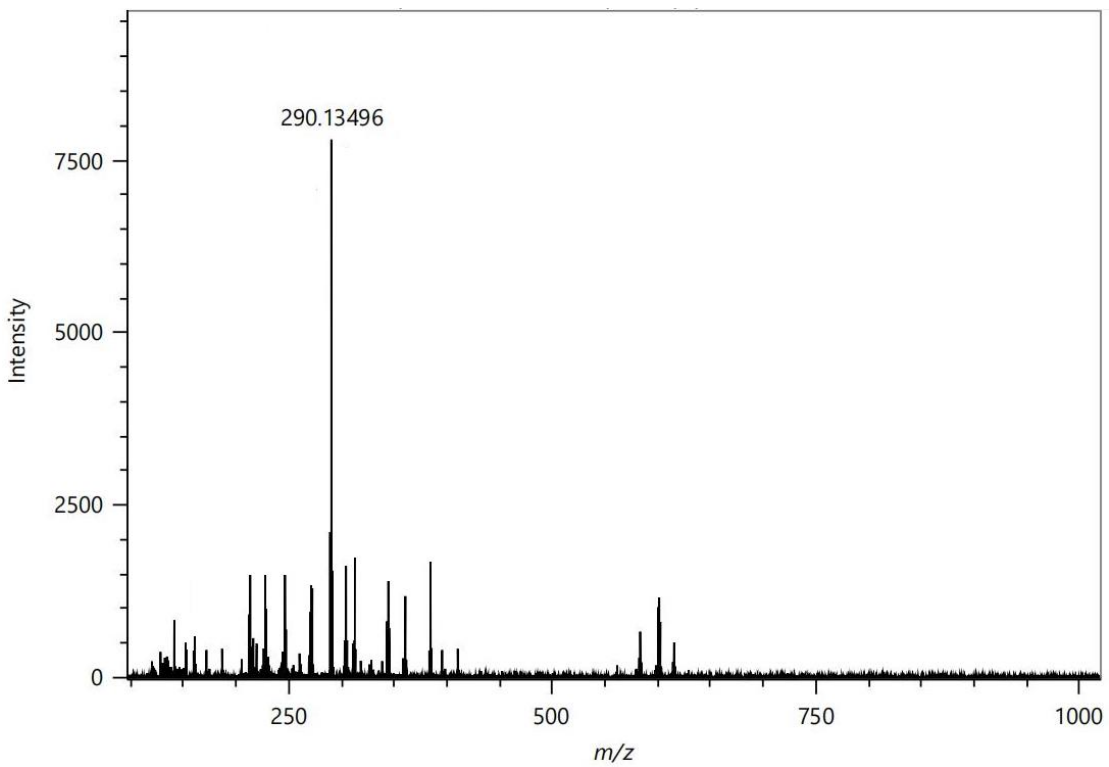

Fig. S6 HR mass spectrum of Compound 2. MS (ESI): m/z 290.13496 $[M+H]^+$.

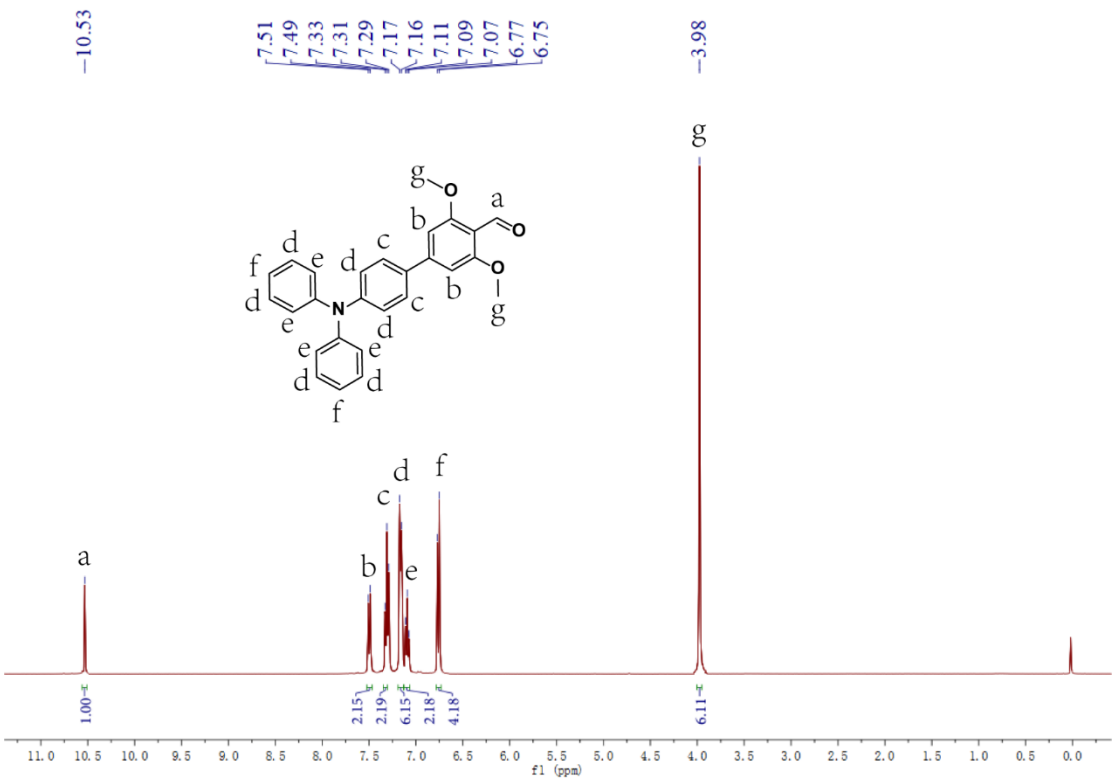

Fig. S7 ^{1}H-NMR spectrum of Compound 3 in $CDCl_3$.

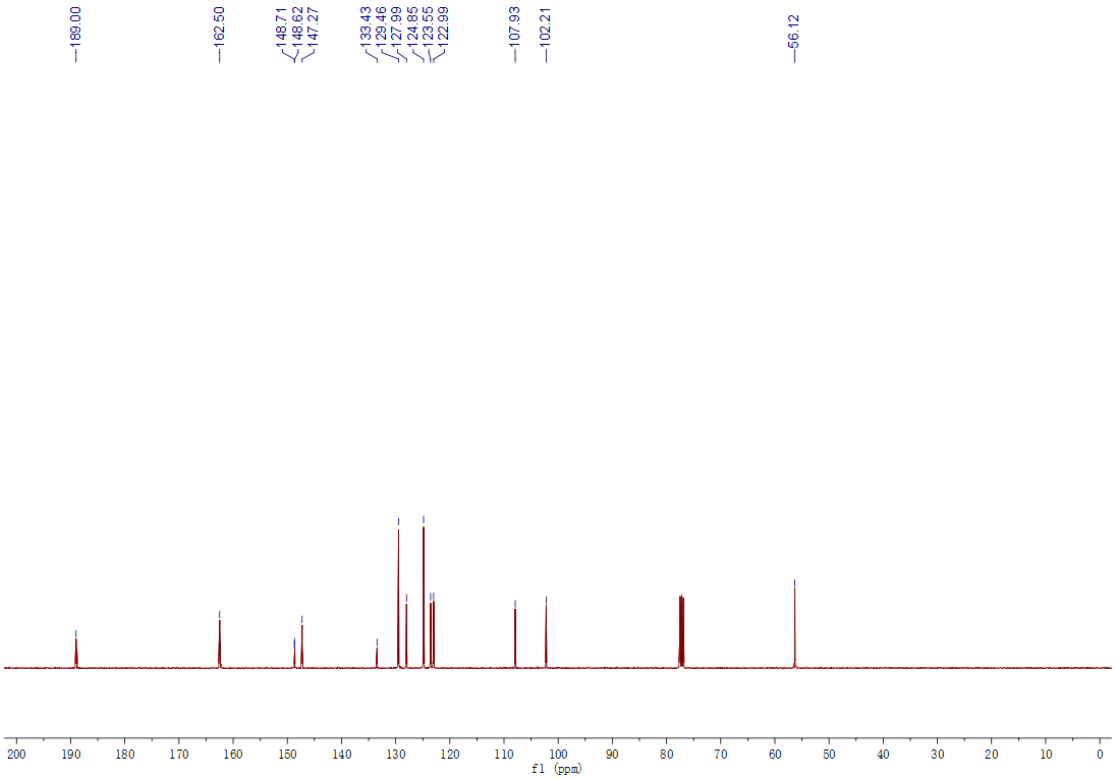

Fig. S8 ^{13}C-NMR spectrum of Compound 3 in $CDCl_3$.

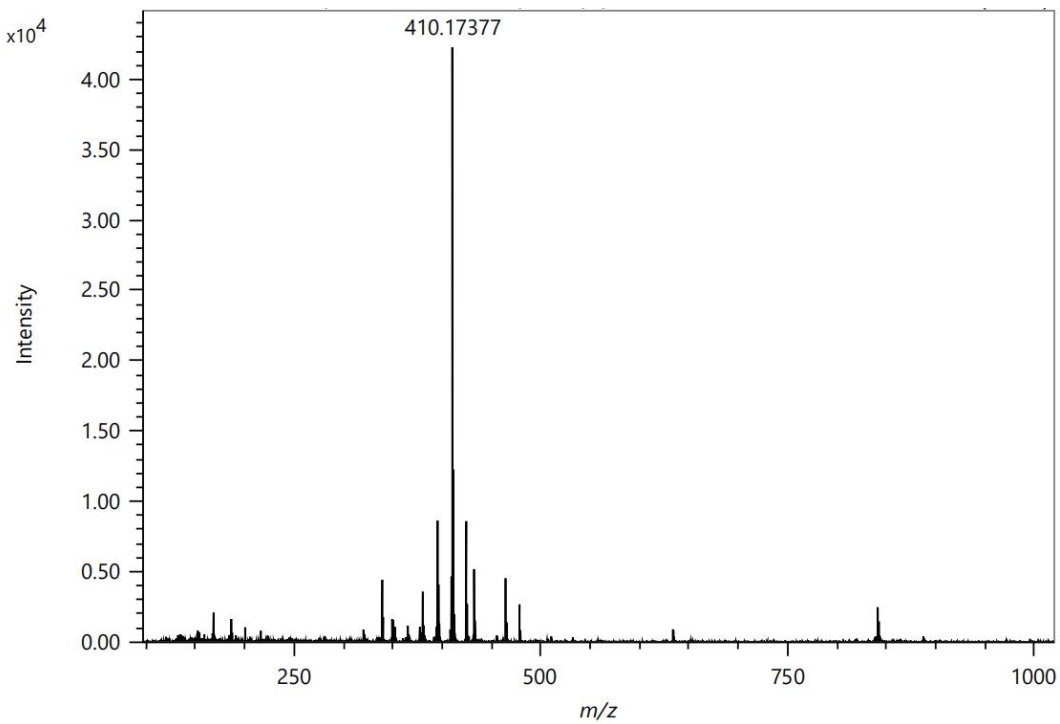

Fig. S9 HR mass spectrum of Compound 3. MS (ESI): m/z 410.17377 $[M+H]^+$.

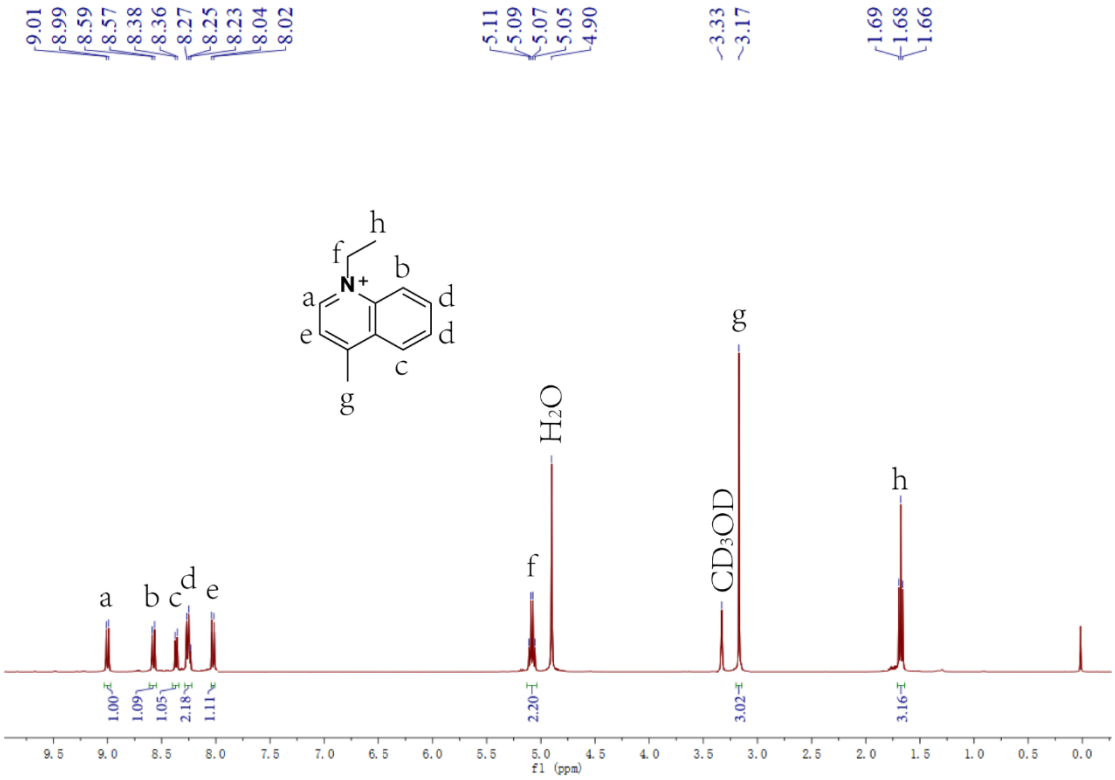

Fig. S10 ^{1}H-NMR spectrum of Compound 4 in CD_3OD.

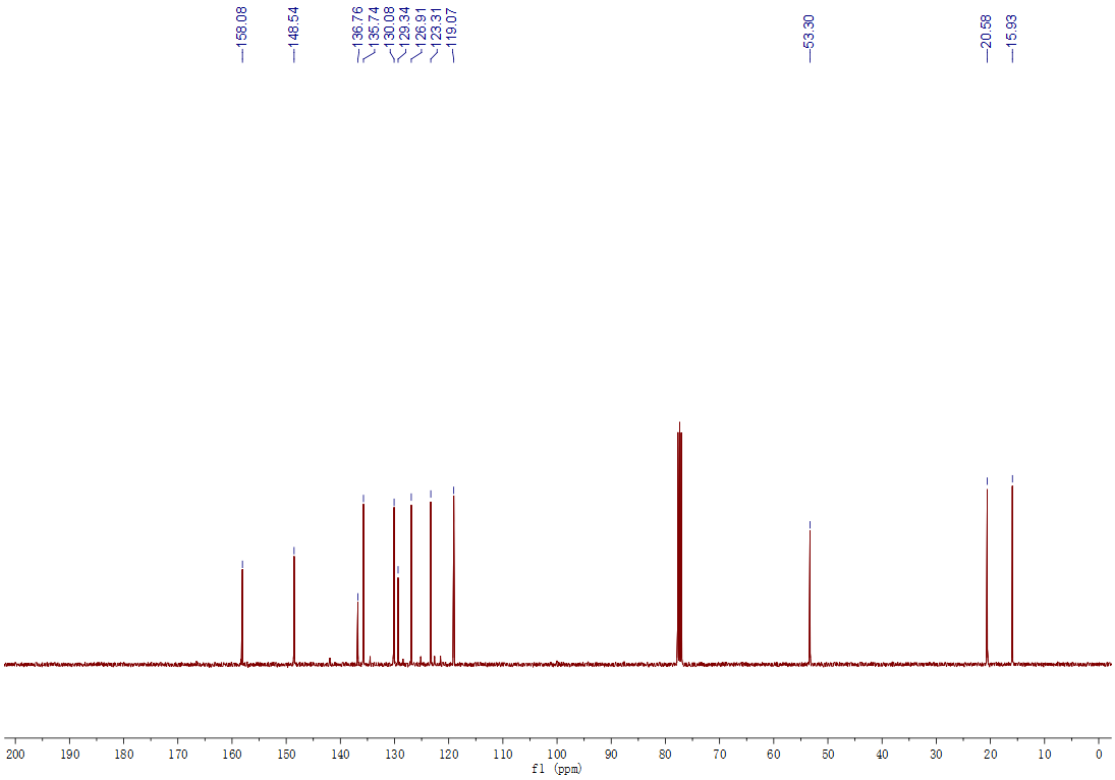

Fig. S11 ^{13}C-NMR spectrum of Compound 4 in $CDCl_3$.

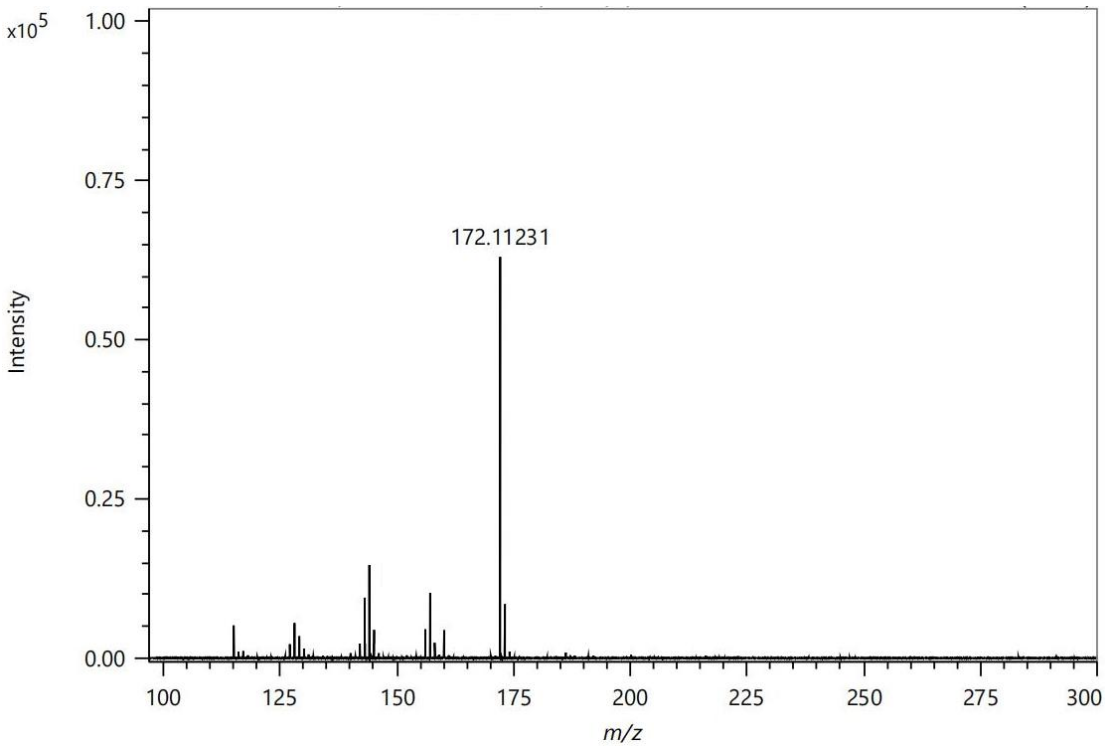

Fig. S12 HR mass spectrum of Compound 3. MS (ESI): m/z 172.11231 $[M]^+$.

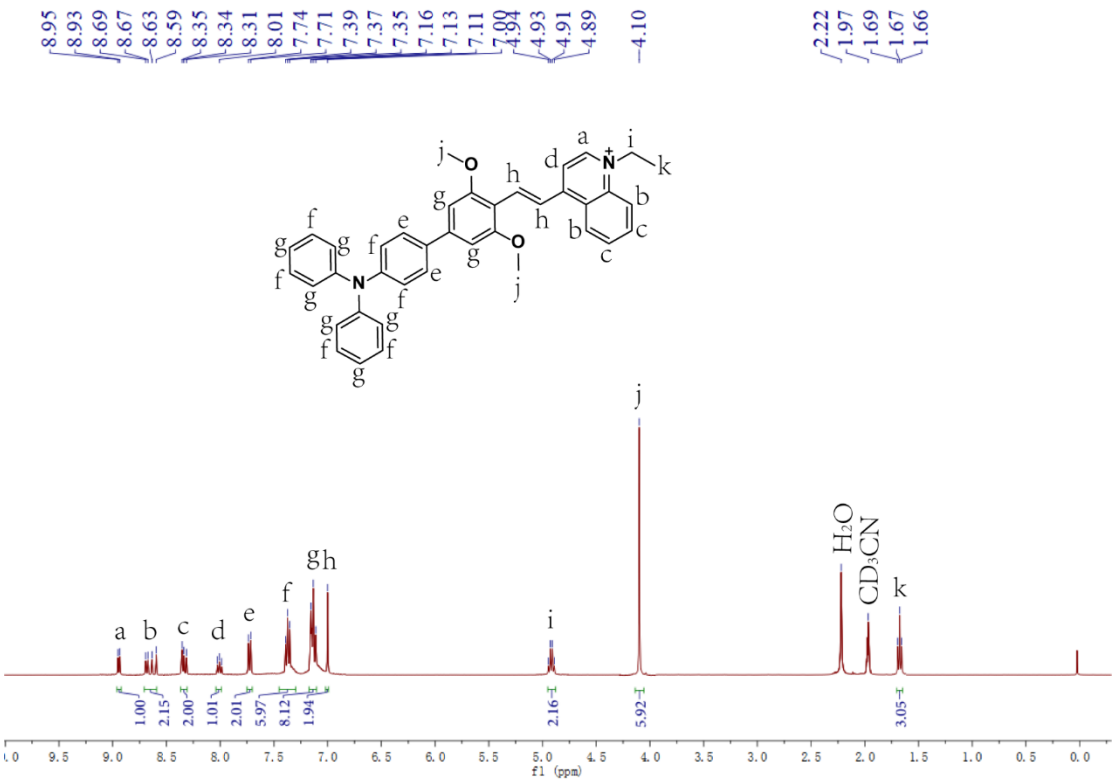

Fig. S13 ^{1}H-NMR spectrum of molecular rotor DPADQ in CD_3CN.

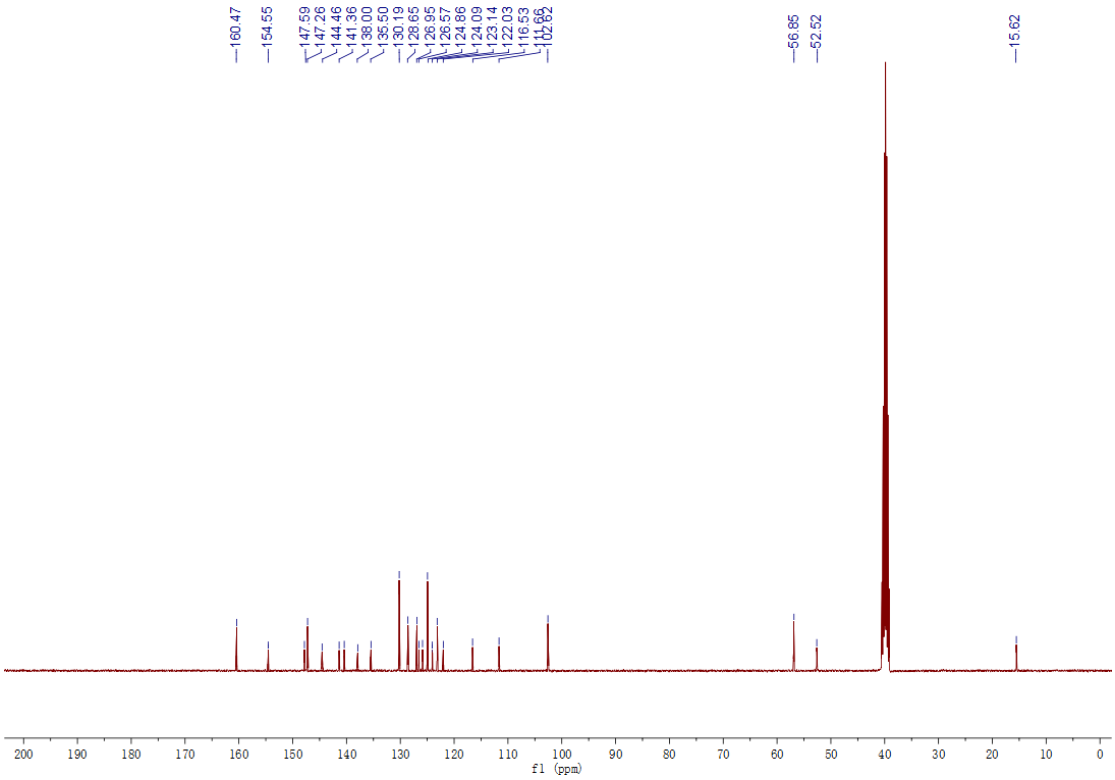

Fig. S14 ^{13}C-NMR spectrum of molecular rotor DPADQ in DMSO-d_6.

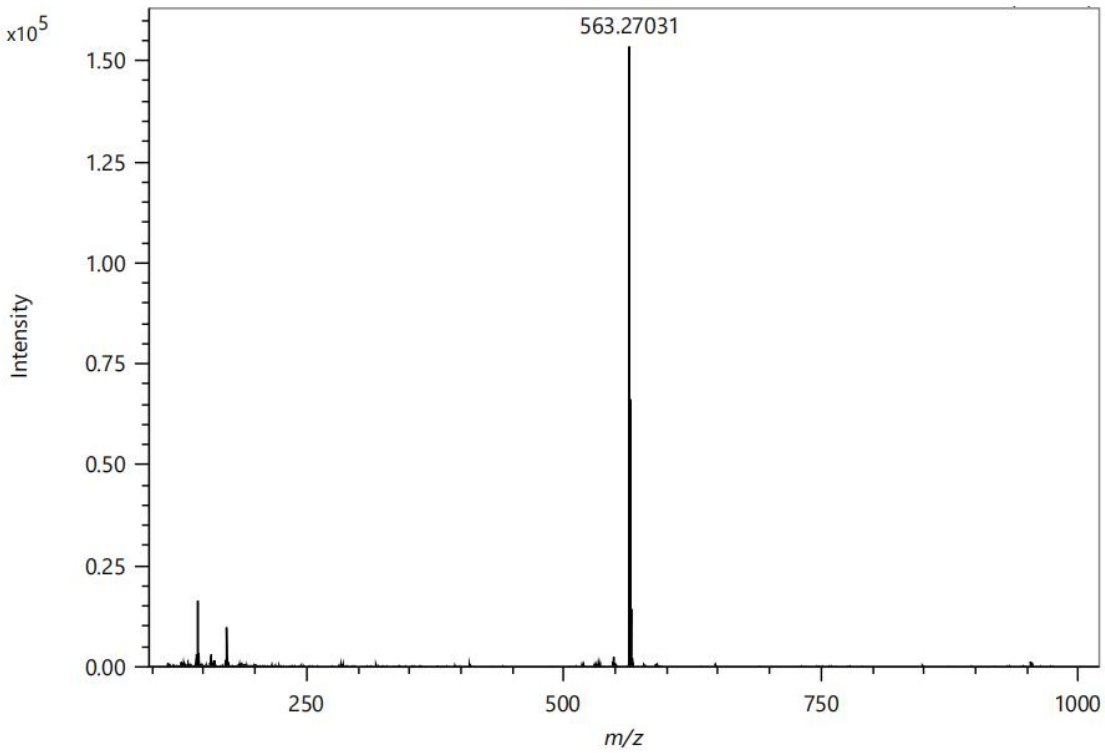

Fig. S15 HR mass spectrum of molecular rotor DPADQ. MS (ESI): m/z 563.27031 $[M]^+$.

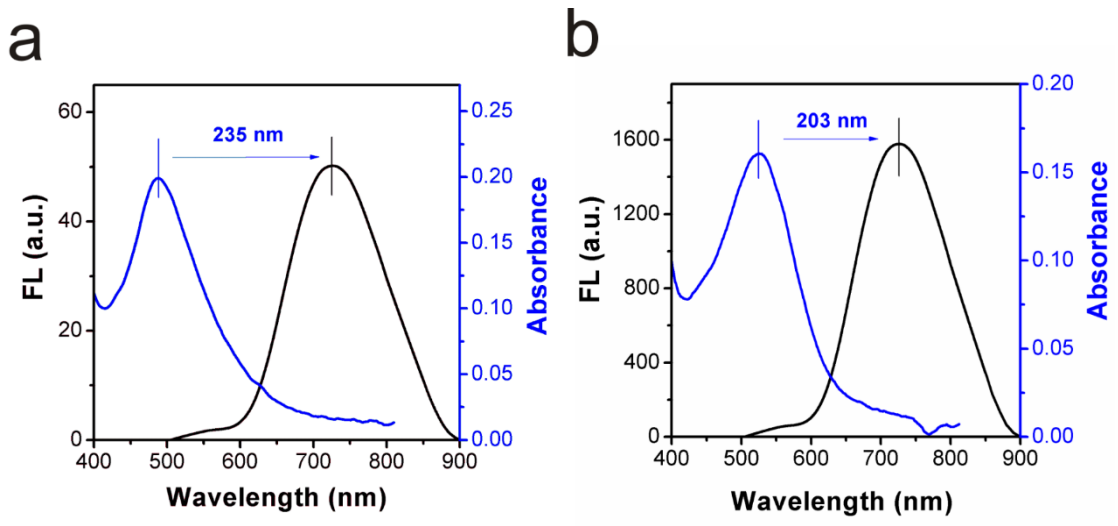

Fig. S16 (a) Fluorescent spectrum (black curve) and absorption spectrum (blue curve) of the molecular rotor DPADQ in water (containing 1% DMSO). **(b)** Fluorescent spectrum (black curve) and absorption spectrum (blue curve) of the molecular rotor DPADQ in glycerol (containing 1% DMSO).

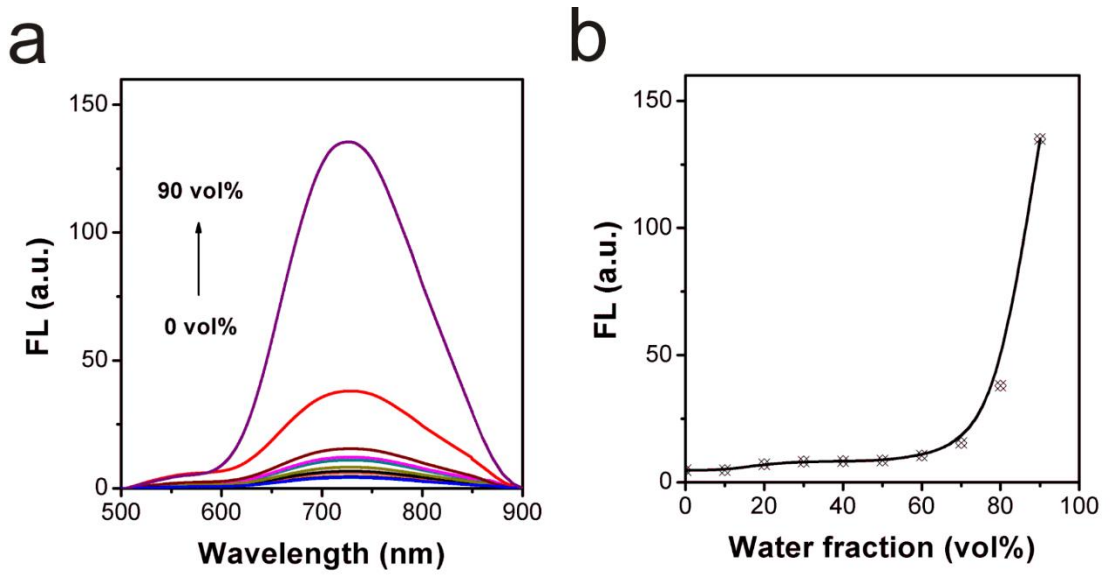

Fig. S17 (a) Fluorescent spectrum of the molecular rotor DPADQ (10 μM) in THF/water with different volume fractions of water (from 0% to 90%). (b) Plot of fluorescence intensity at 725 nm as a function of different volume fractions of water, λ_{ex}=500 nm.

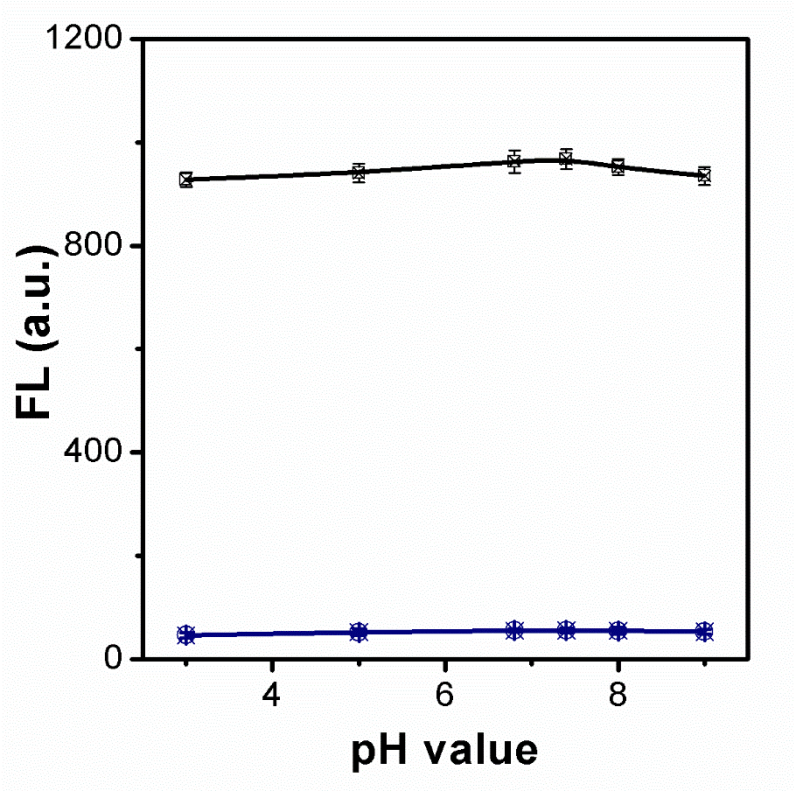

Fig. S18 Fluorescence emission intensity of the molecular rotor DPADQ (10 μM) at 725 nm under various pH values (containing 1% DMSO) in low viscosity environment and in high viscosity environment (90% glycerol), λ_{ex}=500 nm.

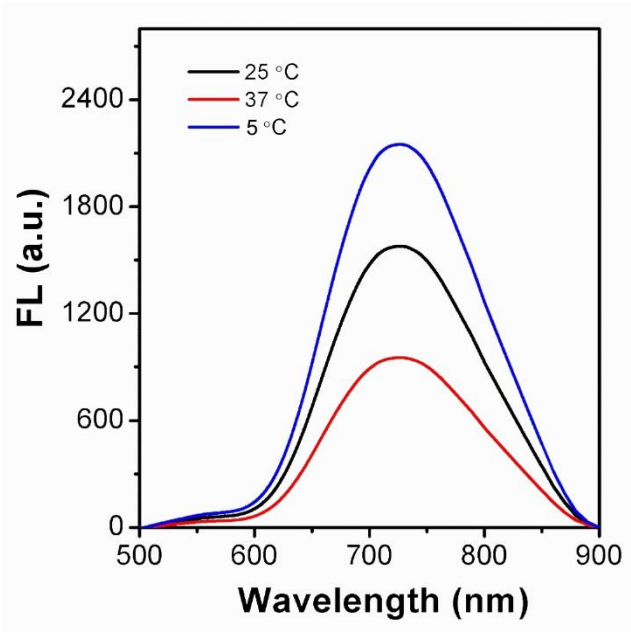

Fig. S19 Fluorescence spectra of the rotor DPADQ (10 μM) in glycerol under different temperature, including the ambient temperature (25 °C), normal body temperature (37 °C), and fresh-keeping temperature (5 °C).

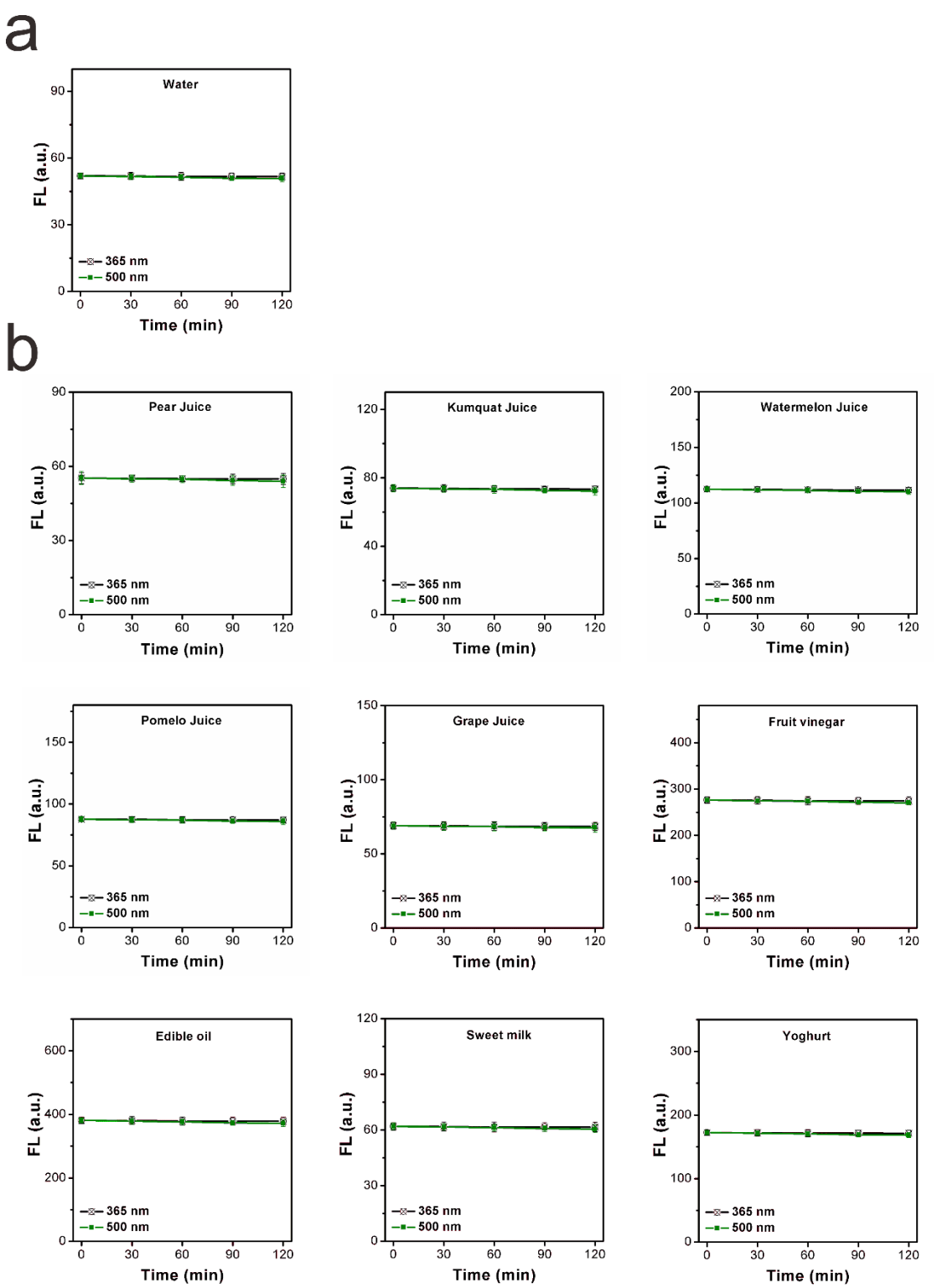

Fig. S20 Photostability analysis of the molecular rotor DPADQ in (a) water (containing 1% DMSO) and other nine kinds of common liquid food (containing 1% DMSO). All upon samples were tested under continuous light irradiation with 365 nm and 500 nm UV lamp.

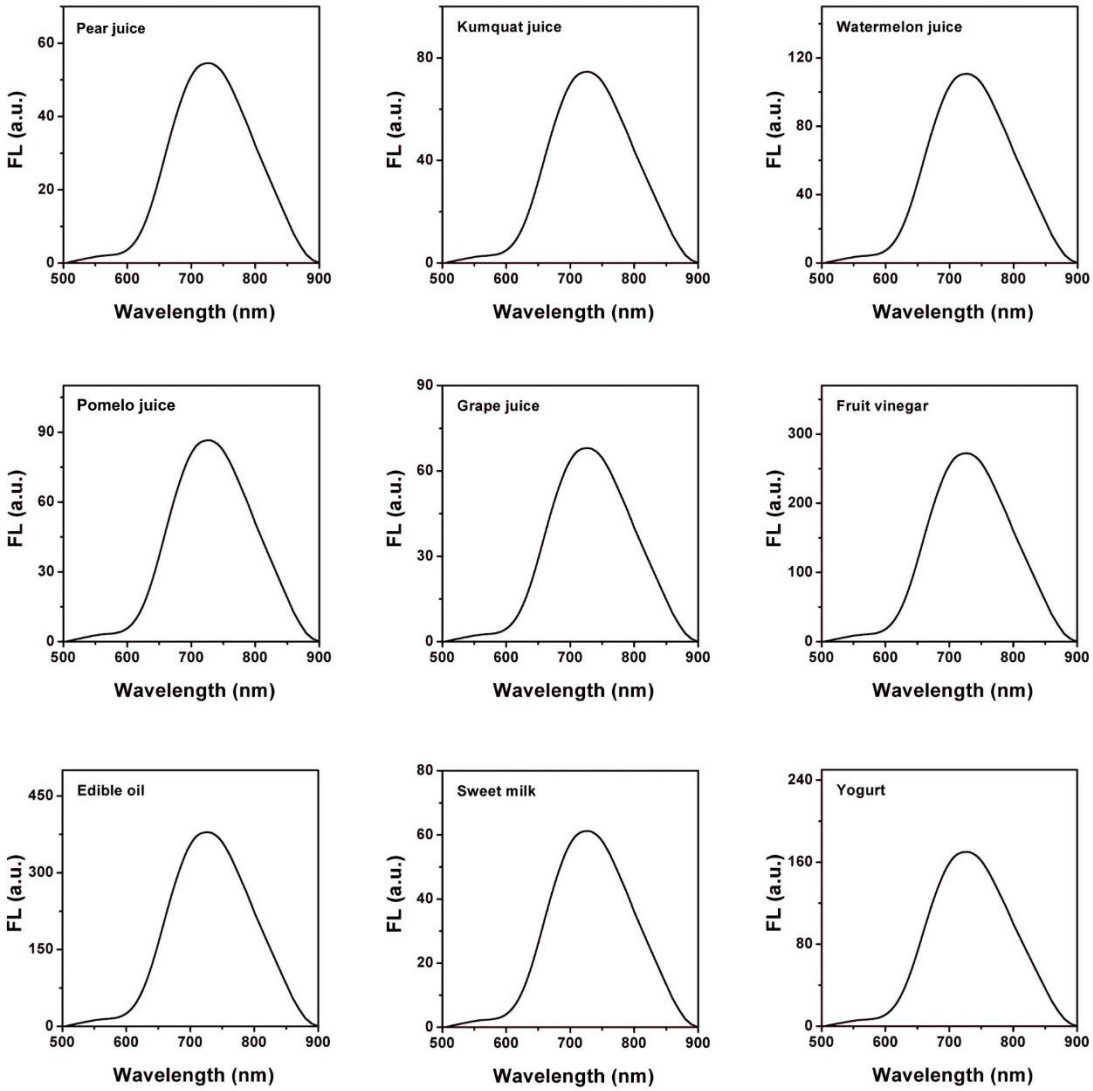

Fig. S21 Fluorescence spectra of the molecular rotor DPADQ (10 μM, containing 1% DMSO) in nine kinds of common liquid food, including the pear juice, kumquat juice, watermelon juice, pomelo juice, grape juice, fruit vinegar, edible oil, sweet milk, and yogurt, λ_{ex}=500 nm.

Table S1. Comparison of the representative fluorescence-based dyes for viscosity detection reported in recent years.

Probe	λ_{ab}*	λ_{em}**	Stokes shift***	Application	Reference
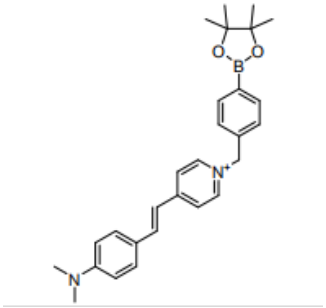	500 nm	607 nm	107 nm	Biological system, living cells.	2
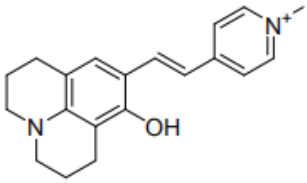	530 nm	620 nm	90 nm	Biological system, living cells.	3
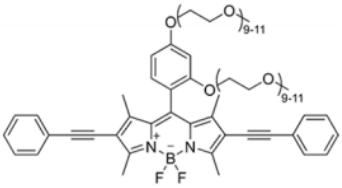	560 nm	580 nm	20 nm	Biological system, living cells.	4
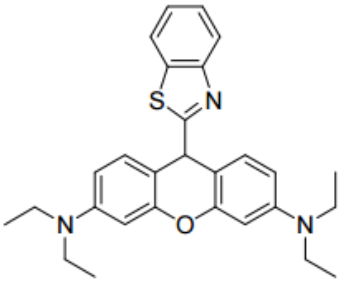	600 nm	635 nm	35 nm	Biological system, living cells, in vivo.	5
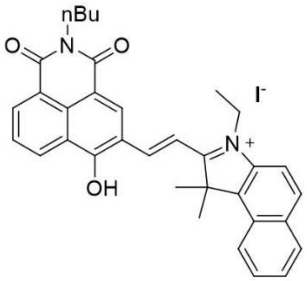	580 nm	635 nm	55 nm	Biological system, living cells.	6
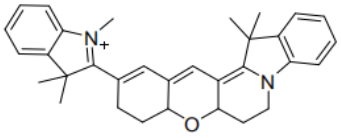	678 nm	698 nm	20 nm	Biological system, living cells, rat slice.	7

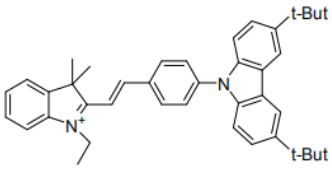	545 nm	628 nm	83 nm	Biological system, living cells.	8
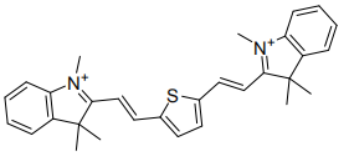	525 nm	595 nm	70 nm	Biological system, living cell.	9
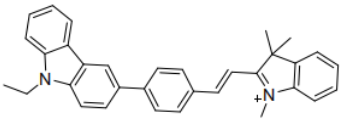	520 nm	610 nm	90 nm	Biological system, living cell, zebra fish, mice.	10
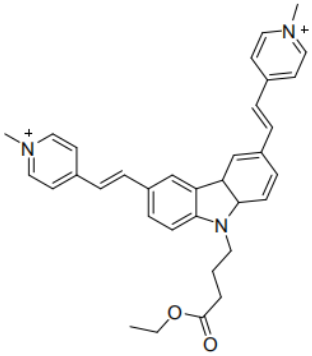	470 nm	560 nm	90 nm	Biological system, living cell.	11
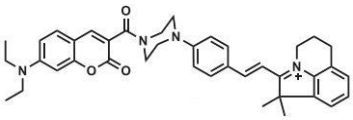	520 nm	580 nm	60 nm	Biological system, living cell.	12
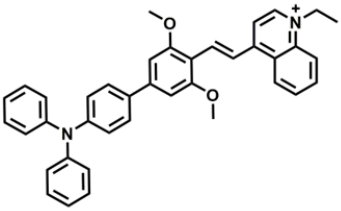	522 nm	725 nm	203 nm	Liquid food, food spoilage analysis.	This work

* Absorption peak. The absorption was measured in the glycerol.

** Emission peak. The fluorescence emission was measured in the glycerol.

*** The stokes shift herein was obtained from the absorption and emission measured in the glycerol.

Table S2. Photo-physical properties of the molecular rotor DPADQ in different solvents.

Solvents	Dielectric constant (ε)	η^* (cP)	Absorption λ_{ab} (nm)	Emission λ_{em} (nm)
Ethanol	24.9	1.2	488.5	/**
Methanol	32.6	0.6	493.1	/
DMSO	46.8	2.1	499.3	/
Acetone	20.7	0.4	484.2	/
THF	7.4	0.5	480.9	/
DCM	8.9	0.4	475.6	/
Ethyl acetate	7.3	0.4	481.5	/
Acetonitrile	37.5	0.4	489.2	/
Glycerol	45.8	956.0	522.0	725.0

* Viscosity of the solvent.

** Non-emissive.

Table S3. Optical properties of the molecular rotor DPADQ in different solvents.

Emitter	λ_{em} (nm)			
DPADQ	Quantum yield in ethanol (Φ)*	Quantum yield in methanol (Φ)*	Quantum yield in DMSO (Φ)*	Quantum yield in Acetone (Φ)*
	0.10%	0.08%	0.12%	0.06%
	Quantum yield in THF (Φ)*	Quantum yield in DCM (Φ)*	Quantum yield in ethyl acetate (Φ)*	Quantum yield in acetonitrile (Φ)*
	0.05%	0.09%	0.07%	0.08%
	Quantum yield in water (Φ)*	Quantum yield in glycerol (Φ)*		
	0.14%	8.6%		

* Estimated using Rhodamine B as the standard (Φ_F = 50% in ethanol).

Table S4. Viscosity values of the beverages determined by viscometer.

Beverages	Viscosity (cP)	Calculated (cP)
Pear juice	2.00	2.01
Kumquat juice	3.50	3.42
Watermelon juice	7.30	7.26
Pomelo juice	4.50	4.54
Grape juice	3.00	2.90
Fruit vinegar	38.10	38.14
Edible oil	68.20	68.33
Sweet milk	2.44	2.46
Yoghurt	16.00	16.15

References

1. I. E. Steinmark, P. -H. Chung, R. M. Ziolek, B. Cornell, P. Smith, J. A. Levitt, C. Tregidgo, C. Molteni, G. Yahioglu, C. D. Lorenz and K. Suhling, Time-resolved fluorescence anisotropy of a molecular rotor resolves microscopic viscosity parameters in complex environments, *Small*, 2020, **16**, 1907139(1-12).
2. M. Ren, B. Deng, K. Zhou, X. Kong, J.-Y. Wang and W. Lin, Single Fluorescent Probe for Dual-Imaging Viscosity and H_2O_2 in Mitochondria with Different Fluorescence Signals in Living Cells, *Anal. Chem.*, 2017, **89**, 552-555.
3. G. Zhang, Y. Sun, X. He, W. Zhang, M. Tian, R. Feng, R. Zhang, X. Li, L. Guo, X. Yu and S. Zhang, Red-Emitting Mitochondrial Probe with Ultrahigh Signal-to-Noise Ratio Enables High-Fidelity Fluorescent Images in Two-Photon Microscopy, *Anal. Chem.*, 2015, **87**, 12088-12095.
4. L.-L. Li, K. Li, M.-Y. Li, L. Shi, Y.-H. Liu, H. Zhang, S.-L. Pan, N. Wang, Q. Zhou and X.-Q. Yu, BODIPY-Based Two-Photon Fluorescent Probe for Real-Time Monitoring of Lysosomal Viscosity with Fluorescence Lifetime Imaging Microscopy, *Anal. Chem.*, 2018, **90**, 5873-5878.
5. M. Ren, L. Wang, X. Lv, J. Liu, H. Chen, J. Wang and W. Guo, Development of a benzothiazole-functionalized red-emission pyronin dye and its dihydro derivative for imaging lysosomal viscosity and tracking endogenous peroxynitrite, *J. Mater. Chem. B*, 2019, **7**, 6181-6186.
6. L. Zhu, M. Fu, B. Yin, L. Wang, Y. Chen and Q. Zhu, A red-emitting fluorescent probe for mitochondria-target microviscosity in living cells and blood viscosity detection in hyperglycemia mice, *Dyes Pigm.*, 2020, **172**, 107859.
7. S. J. Park, B. K. Shin, H. W. Lee, J. M. Song, J. T. Je and H. M. Kim, Asymmetric cyanine as a far-red fluorescence probe for mitochondrial viscosity, *Dyes Pigm.*, 2020, **174**, 108080.
8. K. Zhou, M. Ren, B. Deng and W. Lin, Development of a viscosity sensitive fluorescent probe for real-time monitoring of mitochondria viscosity, *New J. Chem.*, 2017, **41**, 11507-11511.
9. Y. Baek, S. J. Park, X. Zhou, G. Kim, H. M. Kim and J. Yoon, A viscosity sensitive fluorescent dye for real-time monitoring of mitochondria transport in neurons, *Biosens. Bioelectron.*, 2016, **86**, 885-891.
10. J. Yin, M. Peng and W. Lin, Visualization of Mitochondrial Viscosity in Inflammation, Fatty Liver, and Cancer Living Mice by a Robust Fluorescent Probe, *Anal. Chem.*, 2019, **91**, 8415-8421.
11. Z. Zou, Q. Yan, S. Ai, P. Qi, H. Yang, Y. Zhang, Z. Qing, L. Zhang, F. Feng and R. Yang, Real-Time Visualizing Mitophagy-Specific Viscosity Dynamic by Mitochondria-Anchored Molecular Rotor, *Anal. Chem.*, 2019, **91**, 8574-8581.
12. L. He, Y. Yang and W. Lin, Rational Design of a Rigid Fluorophore–Molecular Rotor-Based Probe for High Signal-to-Background Ratio Detection of Sulfur Dioxide in Viscous System, *Anal. Chem.*, 2019, **91**, 15220-15228.